

Original Research Article

Important Atmospheric Parameters over a Indian Tropical Station using Various Remote Sensing Instruments and a Model

Abstract

To report important atmospheric parameters including, temperature, relative humidity, pressure, wind direction, and wind speed over a tropical Indian station i.e. Gadanki (13.5° N, 79.2° E), we use a high-resolution GPS radiosonde intending to study the fine structures of atmospheric parameters. We also considered the COSMIC Radio Occultation (RO) technique, a regular radiosonde, and the European Centre for Medium-Range Weather Forecasts (ECMWF) model-based data to compute the Atmospheric Boundary Layer Height (ABLH), which was estimated using various analytical methods such as vertical gradient, double gradient and logarithmic gradient. Tropopause heights and their corresponding temperatures were identified based on minimum temperature criteria. Gradient and logarithmic gradient methods could effectively capture ABL heights than the double gradient method.

Keywords: High-resolution GPS Radiosonde; Radio Occultation technique; Tropopause; Atmospheric Boundary Layer Height; Analytical methods

1. Introduction

The important atmospheric parameters such as temperature (T), Relative Humidity (RH), pressure (p), and horizontal winds (both zonal and meridional components) are very much essential, mainly to forecast the weather around the world. These important atmospheric parameters are also being used to study the thermal and dynamical state of the atmosphere, and importantly, their vertical profiles of them are also used in further understanding various other important parameters such as boundary layer height and tropopause height and its associated temperature.

Secondly, ABL heights have a significant influence on air pollution. ABLH is the height above the surface to which air pollutants emitted at or from the surface are diluted by convection or mechanical turbulence within a time scale of about 1 h or less [1]. Various remote sensing instruments have been successfully utilized to study ABL height. Particularly, radiosonde is traditionally used to measure ABLH [2], but measured ABLH are confined to the launch time of radiosondes, which is typically 2-4 times a day. Other remote sensing instruments including, LIDAR [3], wind profilers [4], sodar [5], and ceilometers [6] are routinely used to measure ABLH, both convective and stable ABLH category.

The main advantages of GPS RO products are unprecedented vertical resolution, global coverage, all-weather capability and high accuracy. Though the earth's atmosphere has been monitored with RO techniques including mono-satellite GPS/MET [6], CHALLENGING Mini satellite Payload [7] and Satellite de Aplicaciones Cientificas-C [8], due to their relatively sparse sampling, only seasonal or multiyear phenomena of equatorial waves could be studied. As a boon to the scientific community, the launch of six COSMIC (Constellation Observing System for Meteorology, Ionosphere and Climate) satellites provides an order of magnitude increase in the number of GPS-RO profiles available [9]. It has been estimated that COSMIC satellites provide approximately 12 times higher database than the earlier RO missions and, on average, ~1500-2000 profiles will be available during a day around the globe [10-11]. It is, therefore, expected that the COSMIC constellation will provide a much more detailed analysis of wave structures with higher wavenumbers in the lower atmosphere [12]. COSMIC GPS RO technique has already provided a few significant research results in ionospheric altitudes [13-19].

The present research utilizes high-resolution GPS radiosonde, conventional radiosonde, COSMIC RO technique and ECMWF data to understand various important atmospheric conditions over an Indian tropical station (Gadanki). Added to that, various analytical methods were used to determine ABL height and also presented regional variations of ABL heights using ECMWF data. The organization of this article is as follows: Section 2 contains data analysis methodology. In section 3 we present results and discussion, under which high-resolution GPS radiosonde measurements are presented in section 3.1. Section 3.2 contains temperature and pressure profiles as measured by co-located radiosonde and COSMIC RO techniques. Section 3.3 discusses various analytical methods to determine ABL heights. Conclusions are presented in section 3.

2. Data analysis methodology

For this study, we have considered three days data from 01 July to 03 in July 2018. We have downloaded a high-resolution GPS radiosonde from the website (www.narl.gov.in) of the National Atmospheric Research Laboratory (NARL), Gadanki, India and applied a filter to remove data outliers. On the other hand, COSMIC RO and nearby radiosonde data were archived from the COSMIC Data Analysis and Archive Centre (CDAAC; <https://cdaac-www.cosmic.ucar.edu/cdaac/index.html>).

The spatial and temporal differences between COSMIC and RO locations are around 250 km and 2 hours and if such criteria have not met, we, therefore, omitted such profiles in the analysis. The identification of tropopause has been done based on the minimum temperature criteria, while the identification of ABL height was based on gradient method, in which ABL height determines based on the presence of gradients of temperature and humidity profiles. On the other hand, the double gradient method estimates ABL height by finding the second derivative of the potential profile and this method is more effective one when small gradients do exist in the boundary layer. According to the logarithmic method, ABL height is the altitude where the minimum of the logarithm of the first gradient of potential temperature is found.

3. Results and discussion

3.1 High-resolution GPS radiosonde measurements

Each file of downloaded data contains vertical profiles of temperature (T), humidity (%), pressure (P), wind speed (ws), and wind direction (wd). The above data were measured by NARL between 17:35 and 18:55 local time (LT; UT+0530 hrs) in line with the timings of radiosonde that were sent two times a day at various places of the world.

Various panels of Figures, 1a-1c, show vertical profiles of temperature ($^{\circ}\text{C}$), humidity (g.m^{-3}), pressure (hPa), wind speed (m/s), and wind direction (deg). It is obvious from these Figures that the balloon could reach around 20 km, 23 km, and 30 km respectively on 01, 02, and 03 July 2018. It is obvious that the temperature profile shows almost a near inverted Gaussian-shape response with minimum values (indication of tropopause) at around between 16.5 km and 17.5 km.

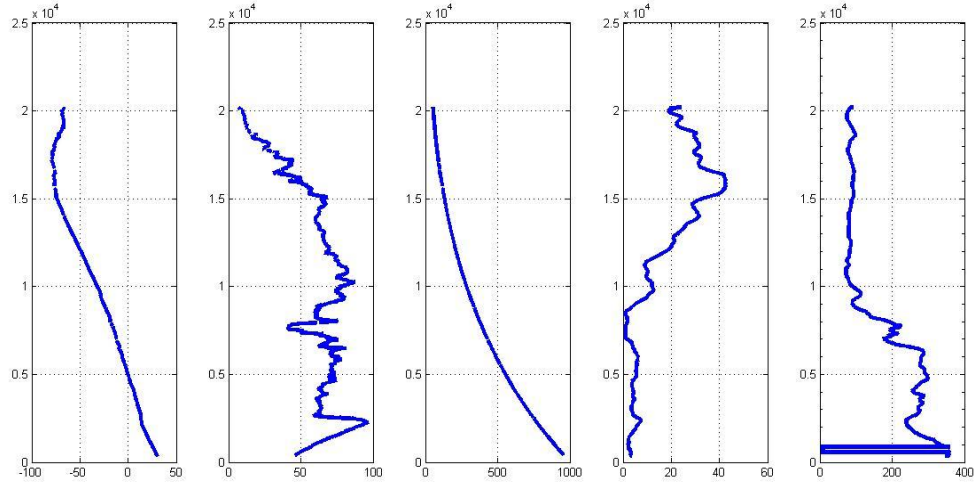


Fig. 1a. Vertical profiles of temperature (extreme left panel), humidity, pressure, wind speed and wind direction (extreme right panel) at 1730 LT over Gadanki on 01 July 2018.

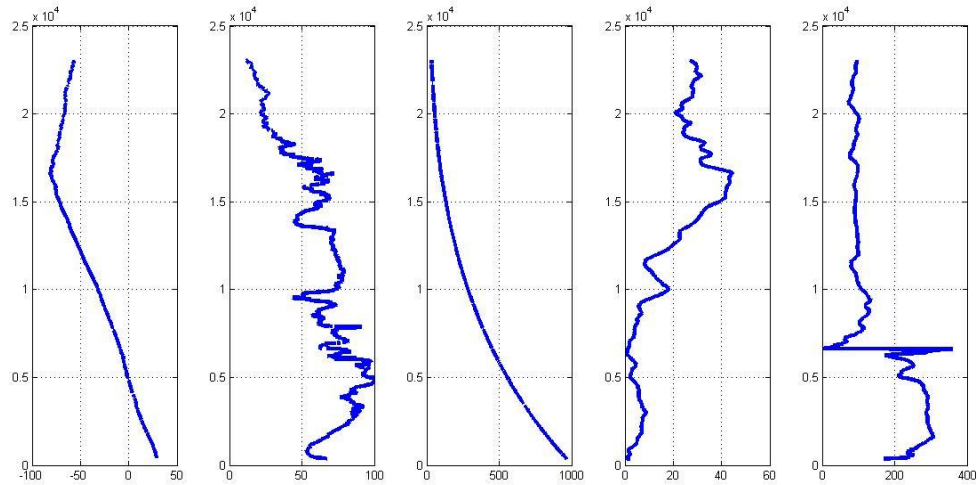


Fig. 1b. Vertical profiles of temperature (extreme left panel), humidity, pressure, wind speed and wind direction (extreme right panel) at 1730 LT over Gadanki on 02 July 2018.

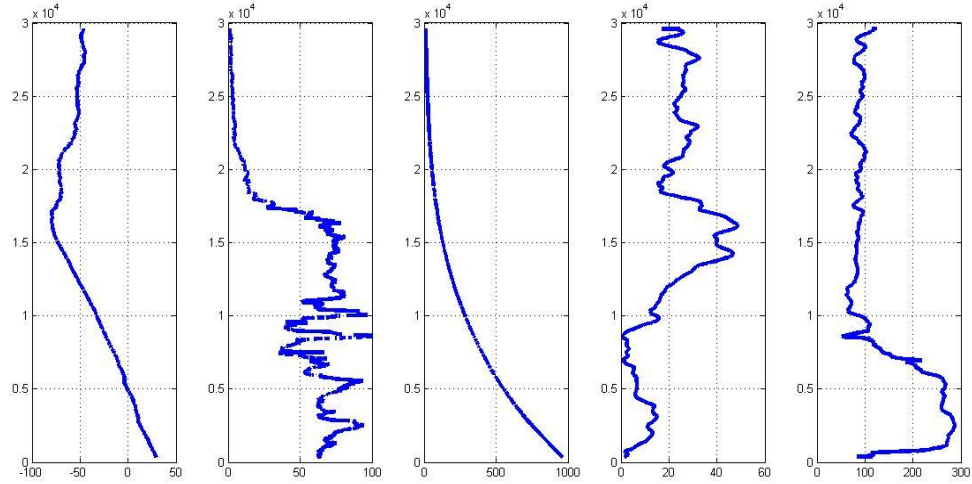


Fig. 1c. Vertical profiles of temperature (extreme left panel), humidity, pressure, wind speed and wind direction (extreme right panel) at 1730 LT over Gadanki on 03 July 2018.

We, therefore, have carefully tabulated tropopause height (in km) and its associated temperatures (in $^{\circ}\text{C}$). Table 1 presents tropopause height measured by RO technique, conventional radiosonde, and GPS radiosonde. The vertical profiles of humidity show very fine structures above 5 km and 15 km altitudes, while pressure profiles show a consistent decrease with the increase of altitude, as expected.

Table 1. Tropopause height (in km) and the corresponding temperature (in $^{\circ}\text{C}$) measured using various remote sensing instruments on 01, 02, and 03 July 2018

Date/ Instrument	01 July 2018		02 July 2018		03 July 2018	
-----	<i>Height (km)</i>	<i>Temp ($^{\circ}\text{C}$)</i>	<i>Height (km)</i>	<i>Temp ($^{\circ}\text{C}$)</i>	<i>Height (km)</i>	<i>Temp ($^{\circ}\text{C}$)</i>
GPS radiosonde	17.24	-79.4	16.59	-81.1	16.51	-80.1
COSMIC GPS RO	16	-76.86	17.3	-80.7	16.8	-78.65
Radiosonde	17.65	-79.25	16.98	-80.6	17.00	-77.25

On the other hand, wind speed and wind directions show different features, which include wind speed appearing to be extremely low below 10 km altitude and a quick look at wind direction shows that most of the winds originated from the north-west

direction, particularly below 5 km altitude. According to Beaufort scale [20], these winds can be categorized as light or gentle breeze category. It is known that light breeze may create an amicable meteorological condition that leads to low- dispersion for air pollutants. However, above 10 km altitude, relatively higher winds (~ 20 m/s or even higher magnitudes above 15 km altitude) are found, whereas wind directions turned southeast directions during all three days.

3.2 Temperature and pressure profiles as measured by co-located RO technique and radiosonde

Figure 2 left (right) panels depict temperature (pressure) profiles between 01 July and 03 July 2018 measured using nearby radiosonde and RO technique. It may be worth mentioning here that radiosonde measurements were taken 200 km and 02:00 hours away from the COSMIC RO satellite locations, which are spatial and temporal distances. Comparisons of temperature and pressure profiles between these two independent techniques reveal a good correspondence [21], however with few following exceptions. There is a slight difference in temperatures measured by these independent observations above the tropopause altitude in all three days. In addition, few differences in magnitudes of temperature are found below, at and near tropopause altitude, in similar lines with earlier studies [22-24].

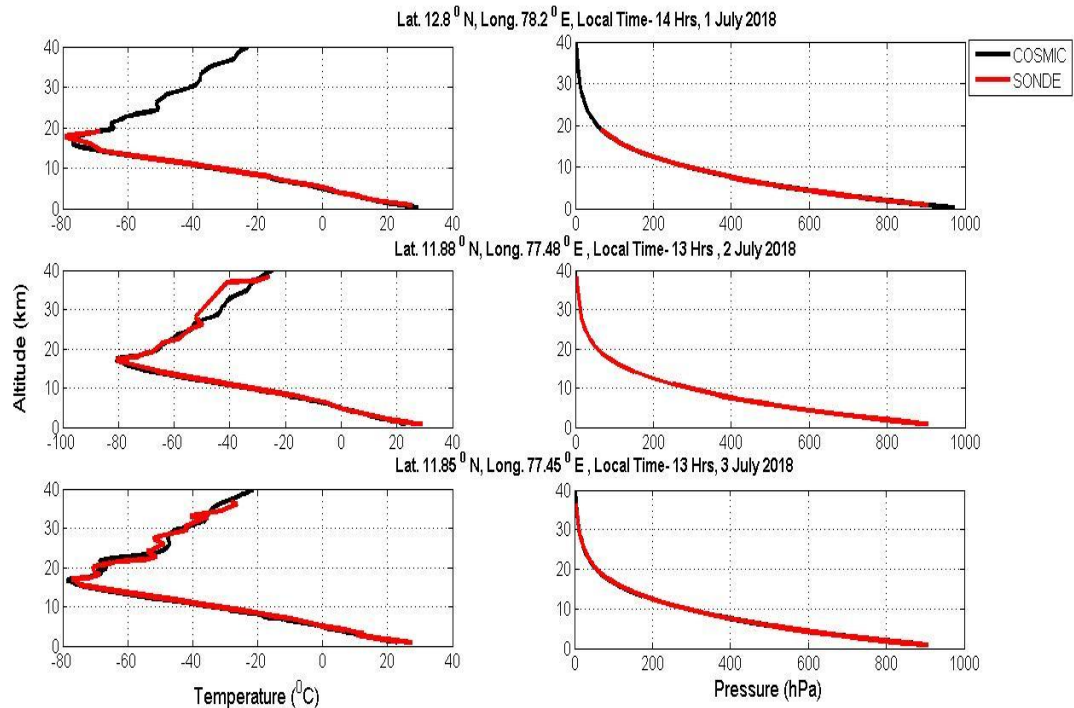


Fig. 2. Vertical profiles of temperature and pressure measured by COSMIC radio occultation technique and radiosonde over nearby locations of Gadanki, India between 01 and 03 July 2018.

For instance, collocated global atmospheric temperature profiles from radiosondes as well as from COSMIC GPS RO satellites were compared for April 2008 to October 2009 and it was found that in the troposphere the temperature standard deviations errors were 0.35 K per 3 h and 0.42 K per 100 km [23]. Comparative studies between GPS RO retrieved temperature profiles from both CHAMP and COSMIC satellites with radiosonde data from 38 Australian radiosonde stations have shown a very good agreement between the two datasets [24]. Specifically, Zhang et al. [24] have found the mean temperature difference between radiosonde and CHAMP to be 0.39°C , while it was 0.37°C between radiosonde and COSMIC satellites. On the other hand, a cent percent consistency in magnitudes of pressure is found. It is, therefore, clear that temperature and pressure profiles show nearly good agreement between these measurements, thereby providing confidence in using COSMIC RO retrieved temperatures in the studies of atmospheric dynamics and tropopause long-term trends.

3.3 Determination of ABL height

The atmospheric boundary layer or Planetary Boundary Layer (PBL) is defined as the lowest part of the atmosphere that is directly influenced by the motions and processes near the Earth's surface²⁵. ABL is one of the important physical characteristics of land-atmosphere communication, and the creation and growth of ABL are linked to surface fluxes such as net radiation and sensible heat. ABL also plays a significant role in various cloud formations, precipitation, and several important feedbacks in the land-atmosphere coupled system [26-27]. This is why the majority of large-scale models have included some representation of the boundary layer processes to simulate a few important climate quantities including, surface dynamics (winds), global cloudiness and precipitation and others [28]. In addition, the transport of lower atmospheric pollutants depends largely on the local atmospheric boundary layer structure. ABLH is one of the important factors affecting pollution concentration and large-scale transport [29]. Thus, ABLH has been used as a key length scale in weather, climate, and air quality models to determine turbulence mixing, vertical diffusion, convective transport, cloud/aerosol entrainment, and atmospheric pollutants deposition [30-32].

We have adopted various analytical methods to compute ABL heights (ABLH) including, gradient, double gradient and logarithmic gradient methods. Figures 3a-3c show various analytical methods and the computed ABLH. Table 2 presents ABL heights measured over nearby locations of Gadanki, India using various analytical methods on COSMIC RO measured data. Both gradient and logarithmic gradient methods show near equal ABLH magnitudes.

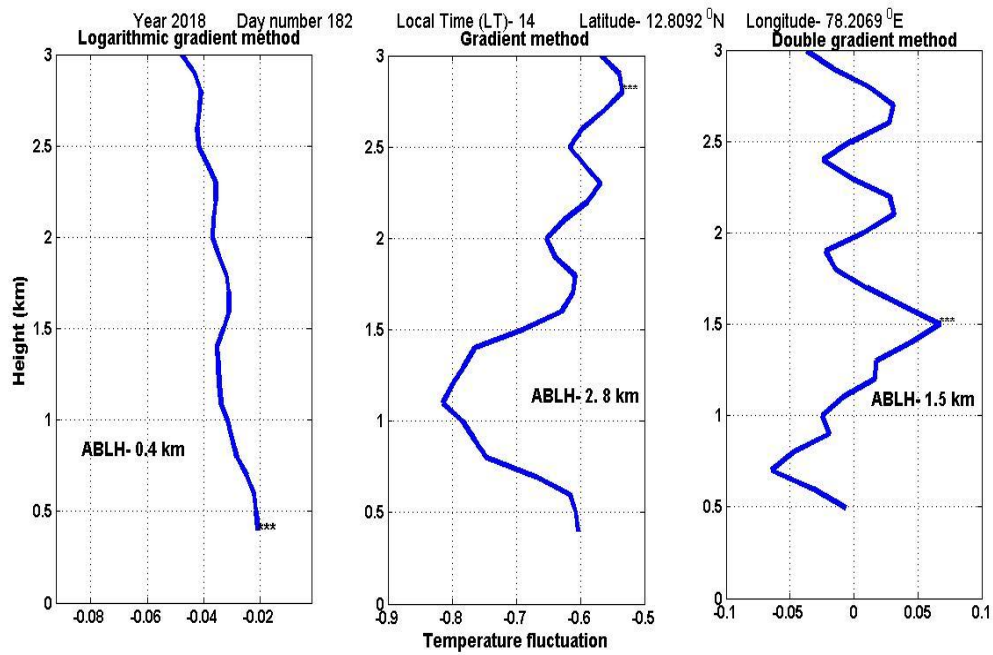


Fig. 3a. Computation of ABLH using various analytical methods over near-by regions of Gadanki on 01 July 2018.

Table 2. ABL height (ABLH in km) in different days of year 2018 measured over nearby locations of Gadanki, India by adopting various analytical methods on COSMIC RO measured data

Date, month and year	Geographical Latitude & Longitude	Logarithmic gradient method	Gradient method	Double gradient method
01 July 2018	12.80 °N 78.20 °E	0.4	2.8	1.5
02 July 2018	11.88 °N 77.48 °E	1.5	3.0	2.0
03 July 2018	11.85 °N 77.45 °E	2.3	2.3	2.2

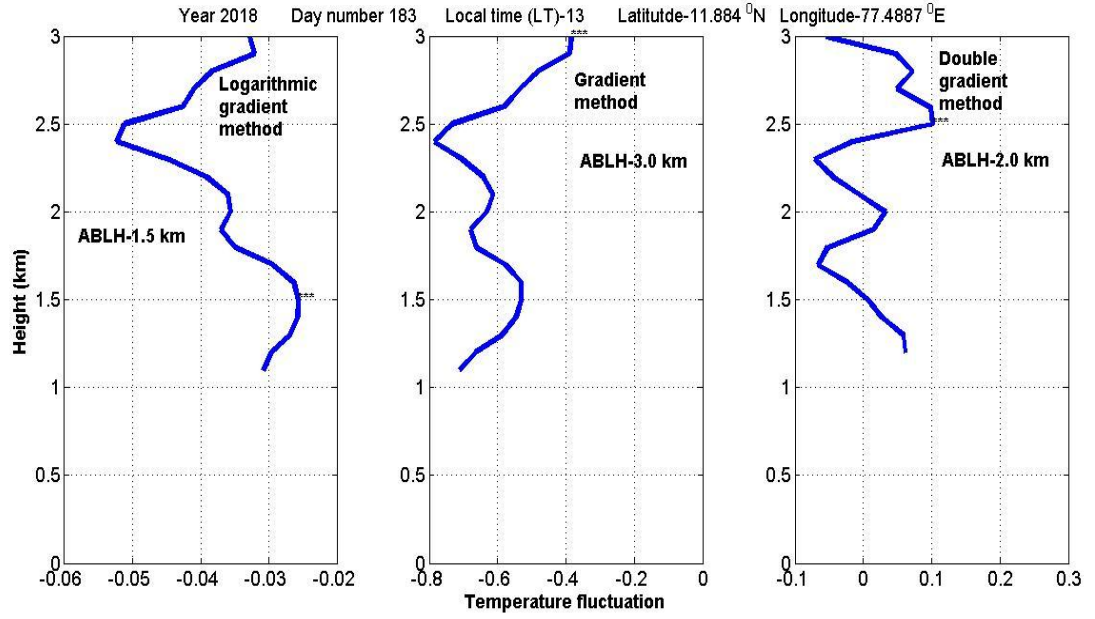


Fig. 3b. Computation of ABLH using various analytical methods over near-by regions of Gadanki on 02 July 2018.

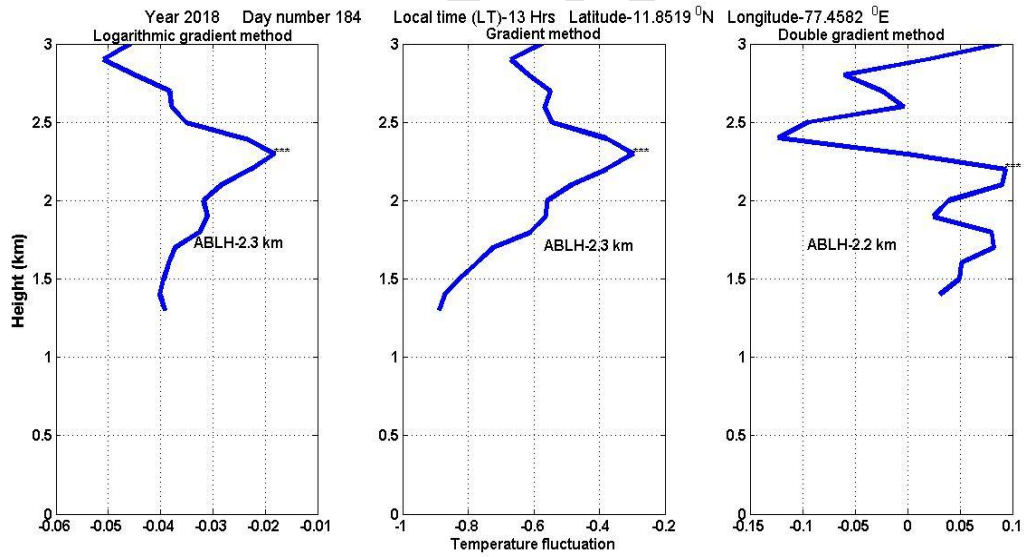


Fig. 3c. Computation of ABLH using various analytical methods over near-by regions of Gadanki on 03 July 2018.

In one of our earlier studies, we have presented global variations of ABLH by using various analytical methods and it is also reported that both gradient and logarithmic gradient methods are better performers in delineating ABL heights [33]. In general, ABL height varies from as low as 100 m under stable conditions and as high as 1500 km under convective conditions [34]. It is, therefore, envisaged that the atmospheric conditions over Gadanki between 01 and 03 come under convective

nature. To verify whether similar magnitudes are associated with ABLH during the same time, we have presented regional trends of ABLH using ECMWF data in the following lines.

We have also presented regional (hourly-based) variations of ABLH in Figure 4 from 1630 LT to 1830 LT between 01 and 03 July 2018. These data were downloaded from the European Union's ECMWF website. It is clear from these figures that land areas recorded the highest values, whereas sea areas are associated with relatively lower magnitudes, as expected. However, land areas have shown significant variations on daily basis. For instance, on 03 July 2018 higher magnitudes are associated with ABLH over Gadanki and nearby locations than the other remaining two days (01 and 02 July 2018), which could be due to higher sensible heat flux [35]. Further, moderate similitude in ABLH magnitudes could be seen between RO measured and ECMEF predicted ones.

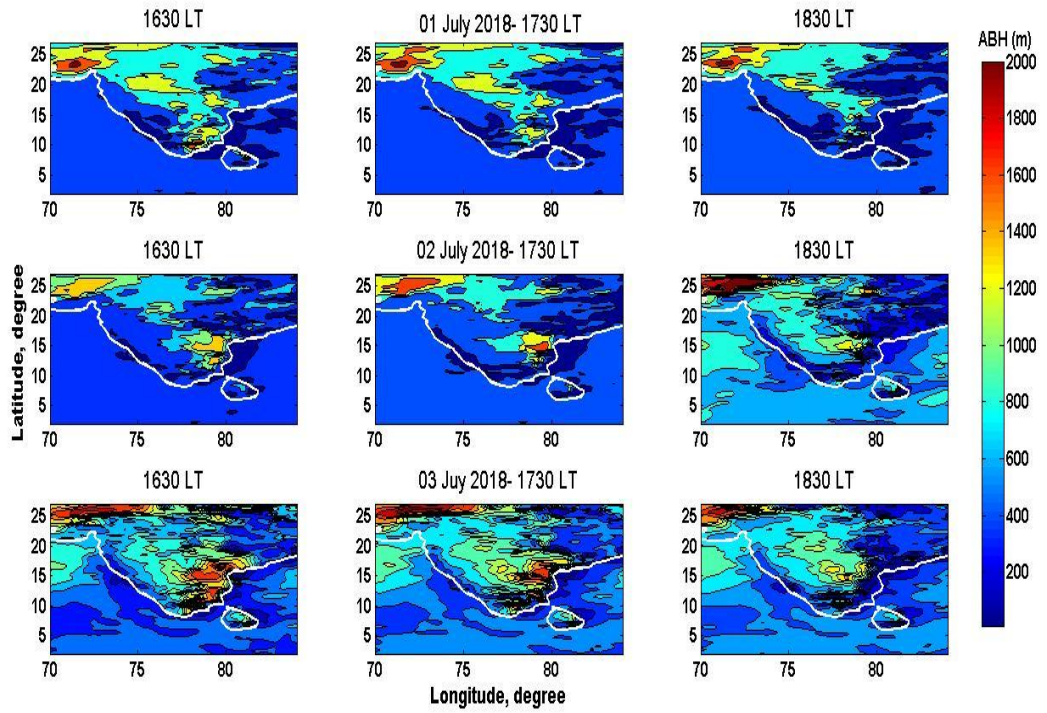


Fig. 4. Hourly (from 1630 to 1830 LT only) variation of ABL heights predicted by the ECMWF model over India and its surrounding areas from 01 to 03 July 2018.

4. Conclusion

The present research considers database from various remote instruments as well as from a famous model. Three various analytical methods were adopted to determine ABL height, whereas most of the earlier studies adhere to a single method or maximum two methods. High-resolution atmospheric measurements are very limited possibly due to costs involved and proper maintenance requirements, particularly in terms of calibration.

The results of this study are:

- a) A great similitude is found in tropopause height measured by high-resolution GPS radiosonde, COSMIC RO technique and conventional radiosonde
- b) Extremely low winds prevailed below 10 km altitude, while relatively higher wind prevailed above 10 km altitude. Winds show north-west directions below 5 km and they turned to south-east directions above 5 km.
- c) Various methods were adopted to calculate atmospheric boundary layer heights using RO retrieved temperature profiles and it is found both gradient and logarithmic gradient could capture boundary layer heights effectively.
- d) Tropopause heights and their corresponding temperatures using various remote sensing instruments are presented that showed great similitude in identifying tropopause heights.
- e) It is, therefore, recommended that multiple databases always reap benefits, particularly in atmospheric studies.

As far as the future scope of this research work is concerned that future research will focus to verify the prowess of various methods (analytical, statistical and wavelet based technique) on huge databases available from the ensuing RO mission and individual station databases available from radiosonde instruments and micrometeorological towers.

REFERENCES

1. Beyrich F. Mixing height estimation from sodar data – A critical discussion. Atmospheric Environment. 1997; 31(23): 3941 - 3953.

2. Seibert P, Beyrich F, Gryning SE, Joffre S, Rasmussen A, Tercier PH. Review and Intercomparison of Operational Methods for the Determination of the Mixing Height. *Atmospheric Environment*. 2000; 34(7): 1001-1027.
3. Cohn SA, Angevine WM. Boundary layer height and Entrainment zone thickness measured by lidars and wind-profiling radars. *Journal of Applied Meteorology and climatology*. 2000; 39(8): 1233 - 1247. Available from
4. Molod A, Salmun H, Dempsey M. Estimating planetary boundary layer heights from NOAA profiler network wind profiler data. *Journal of Atmospheric and Oceanic Technology*. 2015; 32 (9): 1545 - 1561.
5. Martucci G, Milroy C, O'Dowd CD. Detection of cloud-base height using Jenoptik CHM15K and Vaisala CL31 Ceilometers. *Journal of Atmospheric and Oceanic Technology*. 2010; 27(2): 305 – 318.
6. Melbourne, W.G., E.S. Davis, C.B. Duncan, G.A. Haji, K.R. Hardy, E.R. Kursinski, T.K. Meehan, L.E. Young and T.P. Yunck, The application of space-borne GPS to atmospheric limb sounding and global change monitoring. JPL Publ. 94-18, NASA, April, 1994.
7. Wickert, J., C. Reigber, G. Beyerle, R. König, C. Marquardt, T. Schmidt, L. Grunwaldt, R. Galas, T. K. Meehan, W. G. Melbourne, and K. Hocke, Atmosphere sounding by GPS radio occultation: First results from CHAMP, *Geophys. Res. Letters*. 2001; 29, 1187.
8. Hajj GA, Ao CO, Iijima BA, Kuang D, Kursinski ER, Mannucci AJ, Meehan TK, Romans LJ, de la Torre Juarez, Yunck TP. CHAMP and SAC-C atmospheric occultation results and intercomparisons. *Journal of Geophysical Research*. 2004; D06109: 1-24.
9. Anthes R. A., P. A. Bernhardt, Y. Chen, L. Cucurull, K. F. Dymond, D. Ector, S. B. Healy, S.-P. Ho, D. C. Hunt, Y.-H. Kuo, H. Liu, K. Manning, C. McCormick, T. K. Meehan, W. J. Randel, C. Rocken, W. S. Schreiner, S. V. Sokolovskiy, S. Syndergaard, D. C. Thompson, K. E. Trenberth, T.-K. Wee, N. L. Yen and Z. Zenga. The COSMIC/FORMOSAT-3 mission. *Bull. Amer. Meteorol. Society*. 2008; 89: 313-333.
10. Brahmanandam P S, Chu YH, Liu J. Observations of equatorial Kelvin wave modes in FORMOSAT-3/COSMIC GPS RO temperature profiles. *Terrestrial Atmospheric and Oceanic Sciences*. 2010; 21(5): 829–840.
11. Anthes, R. A. Exploring Earth's atmosphere with radio occultation: contributions to weather, climate and space weather, *Atmos. Meas. Tech*. 2011; 4: 1077–1103.
12. Alexander, S. P., T. Tsuda, Y. Kawatani, and M. Takahashi. Global distribution of atmospheric waves in the equatorial upper troposphere and lower

- stratosphere: COSMIC observations of wave mean flow interactions. *J. Geophys. Res.* 2008; 113: D24115.
13. Brahmanandam P S, Chu YH, Liu J. Observations of equatorial Kelvin wave modes in FORMOSAT-3/COSMIC GPS RO temperature profiles. *Terrestrial Atmospheric and Oceanic Sciences.* 2010; 21(5): 829–840.
 14. Brahmanandam P S, Chu YH, Wu KH, Hsia HP, Su CL, Uma G. Vertical and longitudinal electron density structures of equatorial E- and F-regions. *Annales Geophysicae.* 2011; 29: 81–89.
 15. Chu YH, Brahmanandam PS, Wang CY, Su CL, Kuong RM. Coordinated sporadic E layer observations made with Chung-Li 30 MHz radar, ionosonde and FORMOSAT-3/COSMIC satellites. *Journal of Atmospheric and Terrestrial Physics.* 2011; 73(9): 883–894.
 16. Brahmanandam PS, Chu YH, Uma G, Hsia HP, Wu KH. A global comparative study on the ionospheric measurements between COSMIC radio occultation technique and IRI model. *Journal of Geophysical Research Atmospheres.* 2011; 116(A2): A02310.
 17. Brahmanandam P. S, Uma G, Liu JY, Chu YH, Latha Devi N S M P, Kakinami Y. Global S₄ index variations observed using FORMOSAT-3/COSMIC GPS RO technique during a solar minimum year. *Journal of Geophysical Research.* 2012; 117: A09322 1-31.
 18. Uma G, Liu JY, Chen SP, Sun YY, Brahmanandam PS, Lin CH. A comparison of the equatorial spread F derived by the international reference ionosphere and the S₄ index observed by FORMOSAT-3/COSMIC during the solar minimum period of 2007–2009. *Earth Planets and Space,* 2012; 64: 467–471.
 19. Uma G, P. S. Brahmanandam, V.K.D. Srinivasu, D.S.V.V.D. Prasad, V. Sai Gowtam, S. Tulasi Ram and Y.H Chu. Ionospheric responses to the 21 August 2017 great American solar eclipse - A multi-instrument study. *J Advances in Space Research.* 2020; 65 (1): 74 – 85.
 20. World Meteorological Organization. Commission for Maritime Meteorology. The Beaufort scale of Wind Force: (Technical and Operational Aspects). Geneva: WMO, 1970.
 21. Anisetty, S K A V P, P. S. Brahmanandam, G. Uma et al. Planetary-scale wave structures of the earth's atmosphere revealed from the COSMIC observations. *J Meteorol. Res.* 2014; 28; 281–295.
 22. Kishore, P., Namboothiri, S. P., Jiang, J. H., Sivakumar, V., and Igarashi, K.: Global temperature estimates in the troposphere and stratosphere: a validation

- study of COSMIC/FORMOSAT-3 measurements. *Atmos. Chem. Phys.* 2009; 9: 897–908.
23. Sun, B. M., A. Reale, D. J. Seidel, et al., Comparing radiosonde and COSMIC atmospheric profile data to quantify differences among radiosonde types and the effects of imperfect collocation on comparison statistics. *J. Geophys. Res.*, 2010; 115: 684 D23104.
 24. Zhang, K., E. Fu, D. Silcock, et al., An investigation of atmospheric temperature profiles in the Australian region using collocated GPS radio occultation and radiosonde data. *Atmos. Meas. Tech.*, 2011; 4: 2087–2092.
 25. Stull RB. *An Introduction to Boundary Layer Meteorology*. Kluwer Academic Publishers: Germany, 1988.
 26. Betts AK, Ball JH. Budget analysis of FIFE 1987 sonde data. *Journal of Geophysical Research*. 1994; 99 (2): 3655 – 3666.
 27. Margulis SA, Entekhabi D. Boundary-layer entrainment estimation through assimilation of radiosonde and micrometeorological data into a mixed-layer model. *Boundary-Layer Meteorology*. 2004; 110(3): 405-433.
 28. Wentz F J, T Meissner. Atmospheric absorption model for dry air and water vapor at microwave frequencies below 100 GHz derived from space-borne radiometer observations. *Remote Sensing Systems*. 2015; 51: 381– 391.
 29. Coulter, R. L. A comparison of three methods for measuring mixing-layer height. *J. Appl. Meteorol.* 1979; 18: 1495-1499.
 30. Arakawa, A., and W. H. Schubert. Interaction of a cumulus cloud ensemble with the large-scale environment, part I. *J. Atmos. Sci.*, 1974; 31: 674–701.
 31. M J Suarez, A Arakawa and D A Randall. The Parameterization of the Planetary Boundary Layer in the UCLA General Circulation Model: Formulation and Results. *Mon. Weather Rev.* 1983; 111: 2224.
 32. Wesely, M L, D R Cook, R L Hart, R E Speer. Measurements and parameterization of particulate sulfur dry deposition over grass. *Journal of Geophysical Research*, 1985; 90: 213.
 33. Naveen Kumar V, P. S. Brahmanandam, M. Purnachandra Rao, G. Anil Kumar, K. Samatha and L. Rupa Dhanasri, A Study of Atmospheric Boundary Layer (ABL) Height Estimation using Various Analytical Methods - COSMIC RO Measured Temperature Profiles, *Indian J Science and Technology*, 2018; 11(31): 1-12.
 34. Helmis, C.G., et al. A comparative study and evaluation of mixing-height estimation based on sodar-RASS, ceilometer data and numerical model simulations. *Boundary-Layer Meteorology*. 2012; 145(3): 507.

35. P. S. Brahmanandam, V N Kumar, Kumar, G.A. et al. A few important features of global atmospheric boundary layer heights estimated using COSMIC radio occultation retrieved data, Indian J Physics, 2020; 94: 555–563.

UNDER PEER REVIEW